

ESTIMATE OF WELDABILITY OF THE HOT WORK TOOL STEELS VIA THE CCT DIAGRAMS

Dušan Arsić¹ - Vukić Lazić^{1,2} - Ružica Nikolić³ - Branislav Hadzima⁴

Abstract: *Weldability represents a very complex property of a material that shows its ability to form a welded joint of certain characteristics, by application of the adequate welding procedure. It can be determined in several ways. The procedure of weldability estimate, based on the transformation diagrams of continuous cooling (CCT-diagrams) and the measured temperature cycles, is presented in this paper. The objective was to determine the weldability to be able to define the optimal hard-facing technology of the thermo stable steels. The temperature cycles were measured and then the obtained values for the critical cooling time $t_{8/5}$ were entered into the CCT diagrams to estimate the hardness and microstructure of the welded joint's zones. Those two parameters are indicators of the steel's weldability. Experiments were conducted on the multi-layered hard-faced samples made of the steel for manufacturing of the forging dies.*

Keywords: Thermoresistant steels, weldability estimate, hard-facing, temperature cycles, time $t_{8/5}$.

1 INTRODUCTION

Weldability, as a very complex technological material property, can be determined in several ways: theoretically by calculations, in laboratory by experiments, by technological tests and by the Continuous Cooling Transformation (CCT) diagram. Considering the fact that the theoretical determination of weldability does not always have to be reliable, the recommendation is to use some other ways to estimate the material's weldability, as well. Theoretical estimate was very reliable for determination of the cooling time $t_{8/5}$ Ito and Bessyo (1972), since certain output characteristics of the welded joint could be predicted based on that parameter Lazic et al. (2010), (2014a), Arsic et al. (2015a), (2016). However, even that estimate of the critical cooling time in the cited papers was not done purely theoretically, but it was verified by either experimental or numerical investigations. The CCT diagrams could be applied by the similar analogy and constructed for all steels.

The objective of this paper was to point to possibility of the CCT diagrams application for estimate of weldability of the hot work tool steels and their reliability in prescribing the technology for hard-facing of the responsible machine parts. Until now, it was shown that various parts could be repaired by the hard-facing, like forging tools parts Lazic et al. (2014a), Arsic et al. (2015a), (2016), Lazic et al. (2014b), Lazic et al. (2015), , construction mechanization parts Lazic et al. (2011) or the hydro power plants parts Arsic et al. (2014), etc. Here is presented the procedure of using the CCT diagrams to shorten those lengthy and costly experimental procedures. In order to determine the critical cooling time as reliably as possible, it is necessary to record the corresponding temperature cycles. Based on those cycles, the distribution of temperature and heat during

the welding/hard-facing could be monitored Kumar et al. (2014), Zimmer et al. (2009), Murugan et al. (2009), Lan et al. (2015) and the certain temperatures could be related to corresponding structures and characteristics of material in individual zones of the welded joint Galatanu et al. (2014), Arsic et al. (2015b).

2 DETERMINATION OF THE HOT WORK TOOL STEELS TEMPERATURE CYCLES

The temperature cycles measurement was done by thermocouples in the hard-faced plates of the two thicknesses, 7.4 and 29 mm, made of the 56NiCrMoV7 (EN 10027-1). The determined temperature cycles and cooling times were entered into the corresponding CCT diagram and the expected micro structure and hardness of steel were obtained.

Electrodes of the two different diameters d_e , of 3.25 and 4 mm were used for hard-facing and different preheating temperatures and heat inputs were applied, as well. The steel plates of the hot work tool steel were delivered in the tempered condition, with drilled holes for temperature cycles measurement points. The bottom of each hole, into which the thermocouple is being placed, is at a 4 mm distance from the hard-faced layer, i.e. from the welding arc, to secure that the temperature measurements are as accurate as possible. The scheme of the measurement process is shown in Figure 1.

The thermocouple is connected to plotter SERVOGOR S RE 541 Potentiometer recorder, which enables continuous registering of the temperature variation in time. The optimal range of its characteristics (scale type and range, paper speed, etc.) was adjusted.

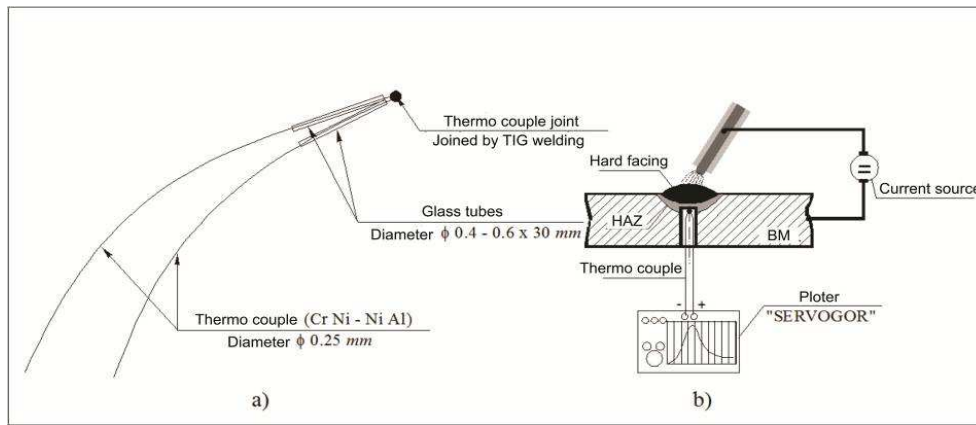


Fig. 1 Scheme of the thermocouple preparation (a) and its position during the hard-facing (b)

The MMA hard-facing parameters are given in Table 1 and present the conditions under which the temperature cycles in the heat affected zone (HAZ) of the hard-faced layer were recorded. In the case of thick plates the stronger current was applied, since it is considered that the source conducts the heat over the volume and not within the plane as in the thin plates Lazić et al. (2010). Different materials were used for

hard-facing and the HAZ was chosen as the measurement point since this is the most critical place in the joint. The given parameters are varying depending on the plates' thicknesses and it is expected that the cooling time between 800 °C and 500 °C to be the longest for the largest heat input or the preheating temperature.

Table 1 Hard-facing parameters

Thickness, s , mm	Electrode diameter, d_e , mm	Hard-facing current, I , A	Working voltage, U , V	Hard-facing speed v_z , mm/s	Heat input, $q_t = \frac{U \cdot I}{v_z} \cdot \eta$, J/mm
7.4	4	140	25.6	1.62-1.36	1765-2110.1
29	5	210	28.5	2.86-0.98	1673.6-4861

The electrode UTOP 38¹ (E Fe 3 according to EN 14700) is aimed for regeneration of parts that operate in the extreme impact pressure loading working conditions.

tables 2 and 3 Lazić et al. (2010), Arsić et al. (2016). The corresponding temperature cycles diagrams are shown in Figures 2 and 3.

¹ UTOP 38 is the notation by the electrode manufacturer SI "Jesenice", Slovenia.

3 EXPERIMENTAL RESULTS

Some of obtained results for the cooling time $t_{8/5}$, determined experimentally and calculated according to three different formulas are presented in

Table 2 Comparative values of the cooling time $t_{8/5}$ ($s = 7.4$ mm, $I = 115$ A, $U = 25$ V, $q_{ef} = 2300$ W)*

Hard-facing speed v_z , mm/s	Heat input q_t , J/mm	Preheating temperature T_o/T_p , °C	Cooling time $t_{8/5}$, s				Point / Layer
			$(t_{8/5})^{I-B}$	$(t_{8/5})^{S_{lim}}$	$(t_{8/5})^{EXP}$	$(t_{8/5})^R$	
2.08	1105.8	180	20.1	84.9	27.00	42-50	18/1
1.90	1210.5	178	22.80	100.3	23.00	48-54	11/1
1.86	1219.2	20	13.34	43.63	16.00	24-26	21/1
1.83	1256.8	178	24.05	107.3	19.00	48.5-57	19/1
1.50	1533.3	180	32.90	163.2	24.50	59-68	2/1

* Notation: I-B – calculated according to Ito-Bessyo formula; S_{lim} – calculated according to limiting thickness, Lazić et al. (2010), R – calculated according to Rikalín's formula, EXP – obtained experimentally

** Shaded fields are the cooling times shown in the CCT diagram in Figure 4.

Table 3 Comparative values of the cooling time $t_{8/5}$ ($s = 29$ mm, $I = 190$ A, $U = 28$ V, $q_{ef} = 4256$ W)

Hard-facing speed v_s , mm/s	Heat input q_l , J/mm	Preheating temperature T_p/T_p , °C	Cooling time $t_{8/5}$, s				Point / Layer
			$(t_{8/5})^J$	$(t_{8/5})^{SER}$	$(t_{8/5})^{EXP}$	$(t_{8/5})^R$	
0.258	16500	204	10.43	14.89	12.0	13.5-14.5	6/1
0.185	23000	235	20.20	37.10	20.5	21-23.5	21/1

For hard-facing of the thin plate ($s = 7.4$ mm) the welding parameters were the following: line energy $ql = 954.3-1691.1$ J/mm, hard-facing speed $vW = 2.41-1.36$ mm/s; preheating temperature $T_p = 20-290$ °C; electrode UTOP 38 - Ø3.25 mm. For hard-facing of the thick plate ($s = 29$ mm) the parameters were: $ql = 1650-3273.8$ J/mm, $vw = 2.58-1.30$ mm/s; $T_p = 20-355$ °C; electrode UTOP 55 - Ø5.0 mm.

Analysis of the obtained temperature cycles has shown that in each diagram one can clearly notice the critical cooling time between 800 and 500°C, what was one of the set experimental tasks. Comparing the diagrams in Figures 2 and 3, the difference in diagrams' appearance, depending on the plate thickness, preheating temperature and quantity of the input heat, can also be noticed. For instance, the maximal temperature T_{max} increases with the input heat for the plate of thickness 7.4 mm, while the maximal temperature for the thick plate (29 mm) is only 906 °C (Figure 3a). The reason for this is the larger mass of the thick plates and faster heat conduction from the heat source towards the periphery.

4 THE HARD-FACING INPUT PARAMETERS INFLUENCE ON THE HARD-FACED LAYERS OUTPUT CHARACTERISTICS

For the 56NiCrMoV7 steel one can find the corresponding TTT (time temperature transformation) and CCT diagrams in manufacturers' catalogues or other reference sources. Those diagrams present the variation of the under-cooled austenite and show the influence of temperature and time on that variation. Though those diagrams were constructed for steel of the certain chemical composition and austenitizing conditions, i.e. in conditions that are different from the hard-facing ones, they can serve in estimates of the output characteristics of the hard-faced layer's zones. This statement was verified several times in various researches of hard-facing.

Considering that this steel belongs into a group of low-alloyed steels with increased carbon content and carbide forming elements (Cr, V and Mo), such a chemical composition itself causes separating of regions of the perlite and bainite transformation, extension of the austenite stability region and lowering the temperature of the martensitic transformation. The CCT diagram for the 56NiCrMoV7 steel is shown in Figure 4.

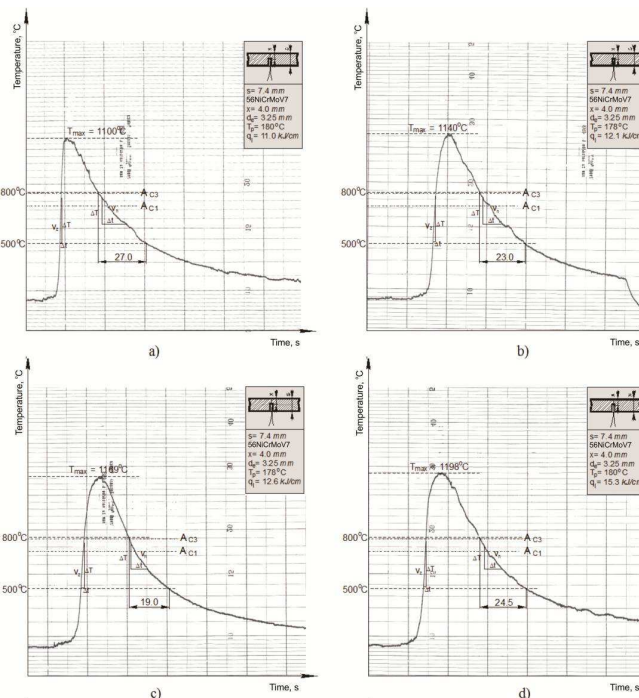


Fig. 1 Temperature cycles in the HAZ of the thin plate ($s = 7.4$ mm)

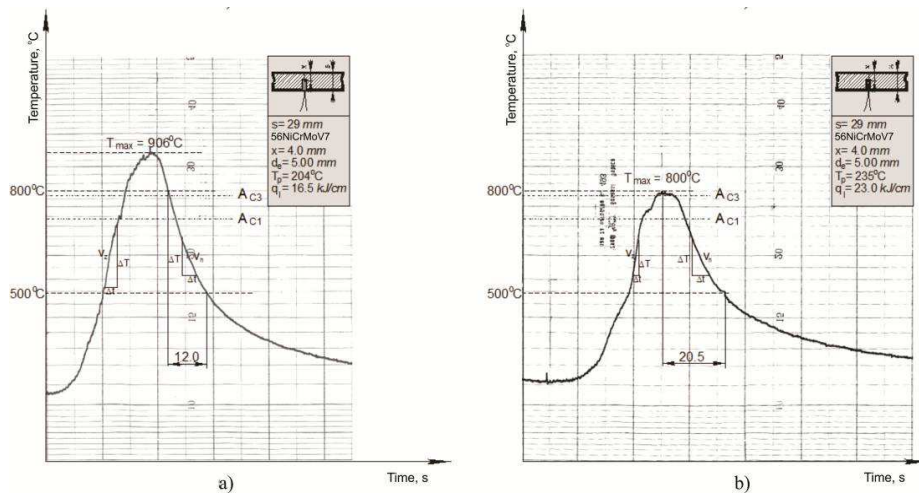


Fig. 3 Temperature cycles in the HAZ of the thick plate ($s = 29 \text{ mm}$)

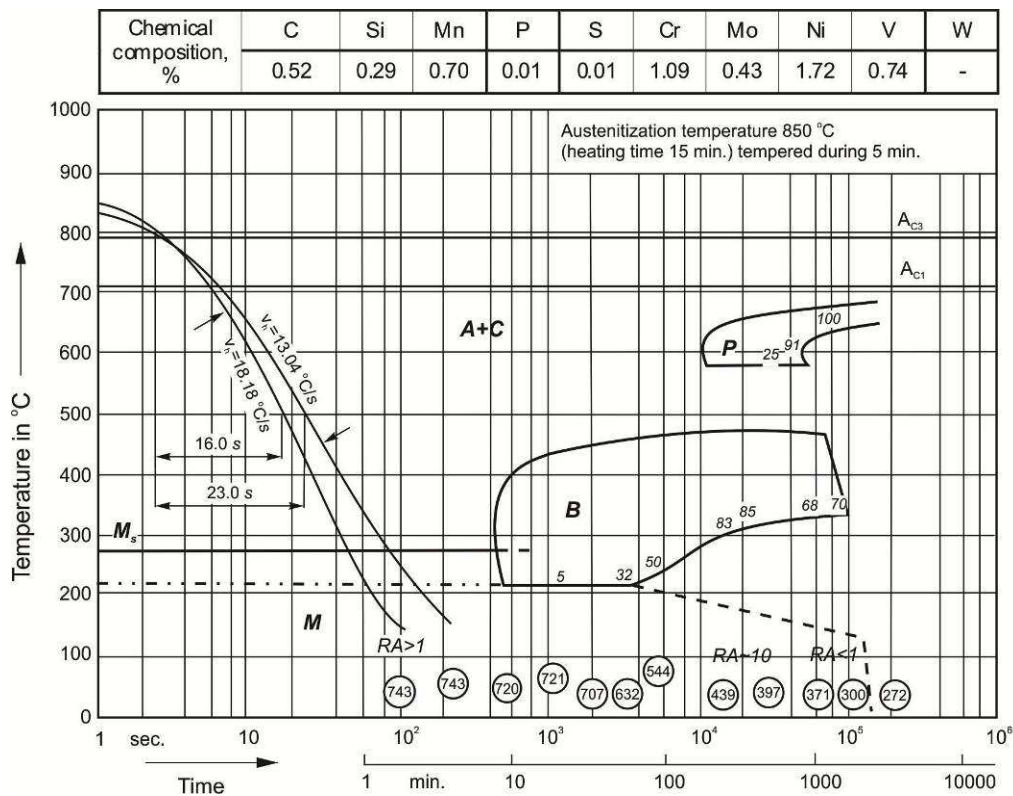


Fig. 4 The CCT diagram for 56NiCrMoV7 steel

From the CCT diagram in Figure 4 one can notice the characteristic temperatures and times of the beginnings and ends of individual phase transformations. Separation of the perlite and bainite transformations in the right-hand part of the diagram is a consequence of the steel's chemical composition, i.e. the alloying elements. Some of the most important characteristics of the applied diagrams, which depend on austenitizing temperature, time of heating and holding on that temperature, grain size, homogeneity of austenite, cooling conditions, and test samples' sizes, are given in Table 4.

Table 4 Austenitizing conditions, critical transformation temperatures and times and maximal hardness, according to different sources

Literature source	$T_{aust.}/t_{transf}$ °C/min	A_{C1} , °C	A_{C3} , °C	M_s °C	t_{100}^* s	t_p^{**} s	HV _m ax
Steel plant "Ravne", Slovenia	860/10	713	798	275	1500	6000	708
Atlas zur wärmebehandlung der stähle	880/15	740	780	250	1050	8000	760
Thyssen Marathon Edelstahl	850/5	715	785	275	500	10000	743

* limiting time that corresponds to the end of the pure martensite structure (for each $t_{8/5} \leq t_{100}$)

** time that corresponds to beginning of the perlite transformation

The newly formed structure and hardness of the HAZ are estimated by entering the cooling time $t_{8/5}$ into the CCT diagram for the given steel. The comparison of structures red-off from the CCT diagrams and structures obtained by the metallographic investigations was performed based on the known cooling curves of some characteristic temperature cycles, Figure 4. From the given diagrams and Table 4, one can notice that the limiting cooling time $t_{8/5} = t_{100}$ ranges between 500 and 1500 s. The limiting cooling time $t_{8/5} = t_{100}$ of approximately 500 s could be obtained with preheating to $T_p = 300$ °C and hard-

facing parameters $q_l = 6$ kJ/mm for the thin plate $s = 7.4$ mm, namely with $q_l = 15$ kJ/mm for the thick plate $s = 29$ mm. These values of the heat input (driving energy) cannot be achieved by the MMA procedure, which means that regardless of the hard-facing input parameters (q_l and T_p) one always obtains the martensite-carbide structure of the HAZ, with hardness between 700 and 743 HV1, Figure 5, Arsic et al. 2015a. Due to that reason one must perform tempering, primarily to reduce the residual stresses and the HAZs hardness and to increase the plasticity of the hard-faced layer's individual zones.

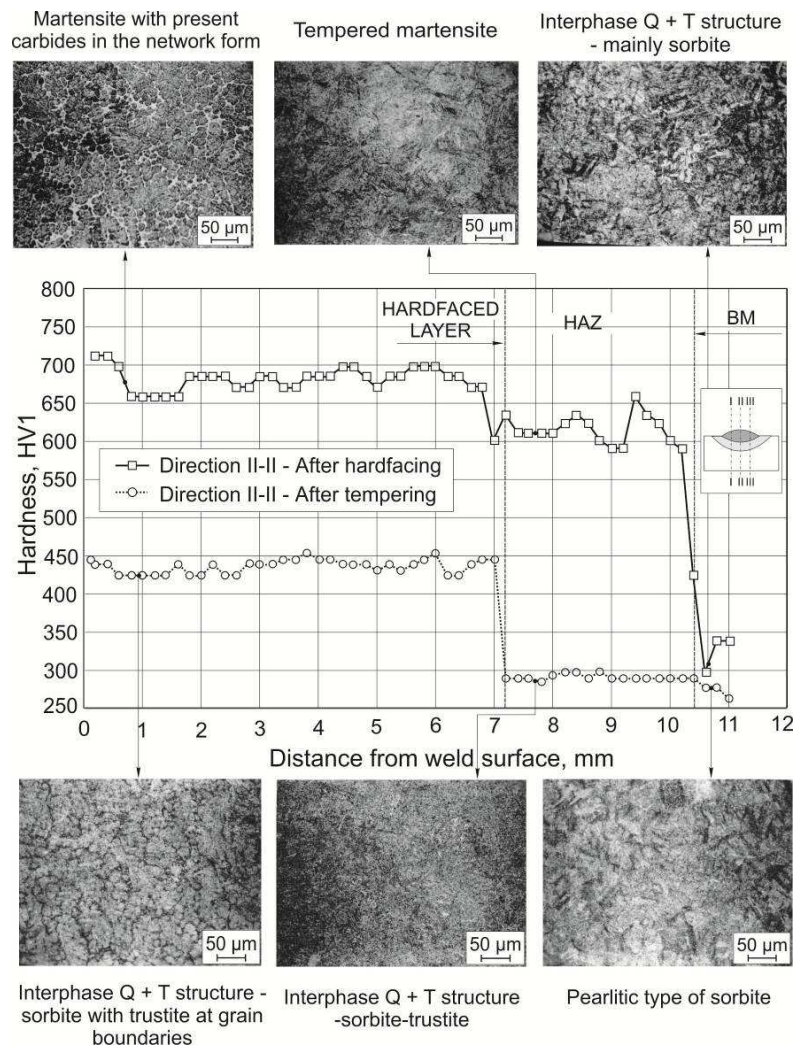


Fig. 5 Hardness distribution and microstructure of the hard-faced layer zones (BM 56NiCrMoV7 – FM UTOP 38 – $s = 7.4$ mm), temperature cycle of Figure 2a.

Tempering exhibits strong influence on properties of this BM hard-faced layers. The hardness

decrease is, on average, greater than 200 HV1, while the significant changes of micro structure were

observed, as well. The martensite with carbides, which is present in the weld metal, transforms after the hard-facing into the more stable phases (sorbite and trustite). Tempering also causes significant decrease of residual stresses Arsić et al. (2015c). This is why one must keep in mind the function of the hard-faced part.

Comparison of results obtained by the CCT diagrams and from experiments shows that there is a high correlation of the hard-facing input parameters and the hard-faced layer's output characteristics, while certain deviations arose from inevitable differences in performing the experiments and obtaining the CCT diagrams.

Obtained results also show that the high tempering of the hard-faced parts must be performed, at a temperature that usually exceeds the working temperature, in order to increase the plasticity, lower the hardness and residual stresses Mutavdžić et al. (2012), Arsić et al. (2015). Results of the hardness distribution and the corresponding micro structures obtained after tempering are shown in Figure 5.

Based on the experimental results it was concluded that the computational cooling time within the critical temperature interval, could be the most accurately obtained by the Ito-Bessyo formula, Ito and Bessyo (1972), Lazić et al. (2010). In that way, the objective of this investigation was reached, since it was shown that the cooling speed can be sufficiently accurately calculated without the expensive experimental procedures. The cooling speed also allows for reading-off the corresponding micro structures and hardness from the CCT diagrams. Knowing the cooling speed and the corresponding transformation diagrams (TTT and CCT) for the considered steel enables approximate definition of the optimal hard-facing technology.

5 CONCLUSION

Based on results presented in this paper, the following conclusions can be drawn:

- Weldability is a complex metallurgical property of materials and for its estimate one should use a combination of different methods.
- Weldability of the hot work tool steels is relatively good, but a series of technological measures must be applied (preheating, post-annealing) to obtain the joint of the favorable properties.
- Measurement of the temperature cycles can be reliably done by use of thermocouples, what is considered as the most accurate method.
- Appearance of the martensitic structure cannot be avoided by varying the process parameters, since the time for martensite forming is too long (≈ 500 s, Figure 4), thus the post-tempering must be done.
- Estimate of the hardness and microstructure of hard-faced/welded joint can be done, with

high reliability, by the CCT diagrams for the given steel, since, as shown for the 56NiCrMoV7 steel in this paper, the hardness red-off from the CCT diagram corresponds to hardness measured on the experimental samples and the micro structure is the tempered martensite, what also corresponds to the CCT diagram.

- The weldability estimate can be reliably done by use of the CCT diagrams and thus the expensive and lengthy experiments can be avoided.

Acknowledgement: *This research was partially supported by the Ministry of Education and Science of Republic of Serbia through Grants TR35024 and OI174004 and by European regional development fund and Slovak state budget by the project "Research Centre of the University of Žilina" - ITMS 26220220183.*

REFERENCES

- [1] Arsić M., Burzić M., Karić R. M., Vistić B., Savić Z. 2014. Methodology for repairing defects on internal surfaces of cranks of guide vane apparatus in hydroelectric generating set at hydropower plant Djerdap 1. *Structural Integrity and Life* 14(2): 121-124.
- [2] Arsić, D., Lazić, V., Nikolić, R., Aleksandrović, S., Djordjević, M., Hadzima, B., Vičan, J., 2015a. Influence of tempering on the deformation level of the multi-layer hard faced samples, *Procedia Engineering* 111: 49-56..
- [3] Arsić, D., Lazić, V., Samardžić, I., Nikolić, R., Aleksandrović, S., Djordjević, M., Hadzima, B. 2015b. Impact of the hard facing technology and the filler metal on tribological characteristics of the hard faced forging dies. *Tehnički Vjesnik-Technical Gazette* 22(5): 1353-1358. Is your business strategy aligned to your Customer needs? Dostupné na: <https://xserveconsulting.wordpress.com/2013/07/27/is-your-business-strategy-aligned-to-your-customer-needs/>
- [4] Arsić, D., Lazić, V., Nikolić, R., Aleksandrović, S., Hadzima, B., Djordjević, M. 2015c. The optimal welding technology of high strength steel S690QL, *Materials Engineering-Materialove inženierstvo* 22(1): 33-47.. - 107 p. – ISBN 978- 3-659-51719-8.
- [5] Arsić, D., Lazić, V., Sedmak, A., Nikolić, R., Aleksandrović, S., Djordjević, M., Bakić, R. 2016. Selection of the optimal hard facing (HF) technology of damaged forging dies based on cooling time $t_{8/5}$. *Metalurgija-Metallurgy* 55(1): 103-106.
- [6] Galatanu, S.V., Faur, N., Pascu, D.R. 2014. Mechanical properties of heat affected zones at macro-microstructural level, using thermal cycle

- simulation, *Structural Integrity and Life* 14(2): 111-114.
- [7] Ito, Y., Bessyo, K. 1972. Weld crackability formula of high strength steels. *Journal of Iron and Steel Institute* 13: 916-930.
- [8] Lan, L., Kong, X., Qiu C. 2015. Characterization of coarse bainite transformation in low carbon steel during simulated welding thermal cycles, *Materials Characterization* 105(7): 95-103.
- [9] Lazić, V., Sedmak, A., Živković, M., Aleksandrović, S., Čukić, R., Jovičić, R., Ivanović, I. 2010. Theoretical-experimental determining of cooling time ($t_{8/5}$) in hard facing of steels for forging dies. *Thermal science* 14(1): 235-246.
- [10] Lazić, V., Mutavdžić, M., Milosavljević, D., Aleksandrović, S., Nedeljković, B. 2011. Selection of the most appropriate technology of reparatory hard facing of working parts on universal construction machinery. *Tribology in Industry* 33(1): 18-27.
- [11] Lazić, V., Aleksandrović, S., Nikolić, R., Prokić-Cvetković, R., Popović, O., Milosavljević, D., Čukić, R. 2012. Estimates of weldability and selection of the optimal procedure and technology for welding of high strength steels, *Procedia Engineering* 40: 310-315.
- [12] Lazić, V., Ivanović, I., Sedmak, A., Rudolf, R., Lazić, M., Radaković, Z. 2014a. Numerical analysis of temperature field during hard facing process and comparison with experimental results. *Thermal Science* 18(1): S113-S120.
- [13] Lazić, V., Nikolić, R., Aleksandrović, S., Milosavljević, D., Čukić, R., Arsić, D., Djordjević, M. 2014b. Application of hard-facing in reparation of damaged forging dies. Chapter 12. In *Analysis of Technology in Various Industries*, S. Borkowski and R. Ulewicz (eds), Association of Managers of Quality and Production, Częstochowa, Poland, 127-143.
- [14] Lazić, V., Arsić, D., Nikolić, R. R., Aleksandrović, S., Milosavljević, D., Djordjević, M., Čukić, R. 2015. Reparation of damaged forging dies by hard facing (HF) technology. *Production Engineering Archives* 6(1): 26-29.
- [15] Murugan, S., Kumar, P.V., Raj, B. Bosc, M.S.C. 1998. Temperature distribution during multipass welding of plates. *International Journal of Pressure Vessel and Piping* 75: 891-905.
- [16] Mutavdžić, M., Lazić, V., Milosavljević, D., Aleksandrović, S., Nikolić, R., Čukić, R., Bogdanović, G. 2012. Determination of the optimal tempering temperature in hard facing of the forging die, *Materials Engineering-Materialove inženierstvo* 19(3): 95-103.
- [17] Rikalin, N. N., *Computations of the thermal process in welding*, Mashgiz, Moscow, 1951.
- [18] Węgrzyn, T., Hadryś, D., Miros, M. 2007. Optimization of operational properties of steel welded structures, *Eksploatacja i Niezawodność-Maintenance and Reliability* 9(3): 30-33.
- [19] Zimmer, K. 2009. Analytical solution of the laser induced temperature distribution across internal material interfaces. *International Journal of Heat and Mass Transfer* 52: 497-503.

AUTHORS ADDRESSES

¹Dušan Arsić

Faculty of Engineering, University of Kragujevac Sestre Janjić 6, 34000 Kragujevac, SERBIA

E-mail: Dusan.arsic@fink.rs

²Vukić Lazić1

Faculty of Engineering, University of Kragujevac Sestre Janjić 6, 34000 Kragujevac, SERBIA

³Ružica Nikolić

Faculty of Engineering, University of Kragujevac Sestre Janjić 6, 34000 Kragujevac
SERBIA

Research Center, University of Žilina Univerzita 8215/1, 010 26 Žilina, SLOVAKIA

E-mail: ruzicarnikolic@yahoo.com

⁴Branislav Hadzima

Research Center, University of Žilina Univerzita 8215/1, 010 26 Žilina, SLOVAKIA